JOURNAL OF Materials CHEMISTRY

Efficient microwave hydrothermal preparation of nanocrystalline anatase TiO_2 colloids

Gregory J. Wilson, Geoffrey D. Will,* Ray L. Frost and Simon A. Montgomery

Centre for Instrumental and Developmental Chemistry, Queensland University of Technology, GPO Box 2434, Brisbane 4001, Australia. E-mail: g.will@qut.edu.au; Fax: 61 7 3864 1804; Tel: 61 7 3864 2297

Received 3rd January 2002, Accepted 18th March 2002
First published as an Advance Article on the web 11th April 2002

Titanium dioxide nanocrystals are an important commercial product used primarily in white pigments and abrasives, however, more recently the anatase form of TiO_2 has become a major component in electrochemical and photoelectrochemical devices. An important property of titanium dioxide nanocrystals for electrical applications is the degree of crystallinity. Numerous preparation methods exist for the production of highly crystalline TiO_2 particles. The majority of these processes require long reaction times, high pressures and temperatures (450–1400 °C). Recently, hydrothermal treatment of colloidal TiO_2 suspensions has been shown to produce quality crystalline products at low temperatures (<250 °C). In this paper we extend this idea utilising a direct microwave heating source. A comparison between convection and microwave hydrothermal treatment of colloidal TiO_2 is presented. The resulting highly crystalline TiO_2 colloids were characterised using Raman spectroscopy, XRD, TEM, and electron diffraction. The results show that the microwave treatment of colloidal TiO_2 gives comparable increases in crystallinity with respect to normal hydrothermal treatments while requiring significantly less time and energy than the hydrothermal convection treatment.

Introduction

The production of titanium dioxide commands a multi-billion dollar industry with over two million tonnes produced each year. The importance of titanium dioxide worldwide is obvious; from its diverse range of commercial applications such as whiteners in paint or as an abrasive in common products such as toothpaste.[1,2] Recently, research into the use of titanium dioxide in photoelectrochemical solar cells has shown considerable promise in generating a cheap route to harnessing solar radiation.[3] Sol–gel processing of titanium dioxide has been investigated since the 19th century and modern processes have been developed to refine and control the stability and phase formation of the colloidal precursors. A range of reaction conditions have been investigated such as the modification of the starting material, variation in the reaction conditions, and the addition of various peptizing agents resulting in the formation of colloidal nanocrystalline anatase particles.[1,2] Subsequent processing through hydrothermal treatment of colloidal TiO_2 suspensions has been shown to produce a high quality crystalline product at low temperatures (<250 °C). The highly crystalline product has been successfully incorporated into electrochemical devices such as electrochromics and photovoltaics where the crystallinity is related to improvements in the desired electrical properties.[3,4] Traditional processes utilised for the formation of nanocrystalline anatase colloids involve the hydrolysis of a titanium alkoxide precursor. Stabilisation of the resulting colloid over several hours with a HNO_3 peptizing agent is followed by hydrothermal treatment in a convection oven for 12–15 hours.

Similarly with respect to the initial formation of the colloidal TiO_2 suspension microwave-hydrothermal synthesis of titanium dioxide has been reported.[5] In contrast to the above product primarily rutile phase colloidal particles were formed. The conclusions drawn from this work were that particle size, morphology, and polymorphism could be controlled by the reaction conditions within the microwave vessel. The main advantages identified were that the microwave-hydrothermal process allowed for rapid heating to temperature and extremely rapid kinetics of crystallisation.[6]

The objective of this research was to determine if changes in crystallinity or phase occur during the convection hydrothermal treatment of titanium dioxide colloidal suspensions. If improvements in crystallinity are seen, then to what extent can this be replicated by the use of microwave-hydrothermal treatment? This work follows the overall aim, driving research into photoelectrochemical solar cells, of producing a device at low cost that will retain the desired electrical properties required for the application.

To understand the importance that titania has to the operation of devices based on its incorporation we consider the dye sensitized photoelectrochemical solar cell (DSC). The DSC is based on a monolayer of charge transfer dye chemisorbed to the surface of a nanoporous nanocrystalline titania substrate. The chemical link formed between the dye and the titania substrate facilitates the transfer of a photoinduced electron from the excited state of the dye molecule into the conduction band of the titania. The original state of the now oxidised dye can be restored through electron transfer from the electrolyte, which typically contains a redox system such as the iodide/triiodide couple.

The photoinduced oxidation of the adsorbed dye molecules results from electron transfer into the titania which are quickly reduced by the species present in solution. This rapid reduction prevents the back electron transfer from the conduction band to the adsorbed dye. The injected electron then migrates through the nanoporous nanocrystalline titania network until it reaches the conducting contact. The electron completes the cycle by travelling through the external load, under the force of the established potential gradient, to the counter electrode where it regenerates iodide through the reduction of triiodide.

The dye sensitised nanoporous nanocrystalline electrodes typically have a large surface area, 1000–2000 times that of the projected surface area. These electrodes are responsible for the initial transport of electrons away from the dye molecules. The transport of electrons through the nanoporous

DOI: 10.1039/b200053a

nanocrystalline titania electrode has been identified as one of the major loss mechanisms in the efficiency of the cell.[7] Improved crystallinity removes potential trap states due to lattice imperfections in the titania nanocrystallites and thus improves conduction through the nanoporous titania electrodes which they form.

Experimental

Colloidal TiO_2 solutions were prepared by hydrolysis of titanium isopropoxide following an experimental procedure adapted from that of O'Regan *et al.*[8]

Briefly, 20.0 cm^3 of isopropanol (AR grade) and 125 cm^3 of titanium isopropoxide (Aldrich AR grade) were accurately measured into a 150 cm^3 dropping funnel. The resulting solution was added over 10 minutes with vigorous stirring to 750 cm^3 of ultra pure deionized water (18.2 MΩ cm) in a 2.00 dm^3 conical flask. On completion of the addition, 5.30 cm^3 of 69% nitric acid (AR grade) was added as a peptizing agent. The solution was immersed in a hot water bath, heated to 80 °C and stirred continuously for 8 hours. Approximately 700 cm^3 of a white colloidal solution (pH 1.2, yield 99% based on TiO_2 weight) remained and was stored in a dark glass vessel.

Convection hydrothermal treatment of nanocrystalline titanium dioxide colloid

A previously described procedure[3,4] was followed to prepare convection hydrothermally treated titanium dioxide. 100 cm^3 of titanium dioxide colloid prepared as above were placed into a 200 cm^3 Pyrex glass lined stainless steel autoclave Parr-bomb. The sample was treated for 15 hours at 200 °C in a convection oven (1300 W, S.E.M.), allowed to cool to room temperature for 2 hours and the suspended product allowed stand for 24 hours.

Microwave hydrothermal treatment of nanocrystalline titanium dioxide colloid

A 30 cm^3 aliquot of titanium dioxide colloid prepared as above was placed into a Teflon lined digestion vessel. From vaporization enthalpy tables, the operating pressure of the microwave reaction vessel operating at 30 psi correlates to 121.5 °C, and 60 psi to 145 °C. A microwave oven (630 ± 50 W, MSD-2000 from C.E.M) was set at 80% power and the pressure ramped from atmospheric to the required pressure (30–60 psi) over a 2 minute period. The duration of treatment was also varied from 5–10 minutes.

All TiO_2 samples were divided equally and one half dehydrated in an oven for 3 hours at 80 °C to allow analysis of the product.

Raman spectra were recorded for the bulk crystalline material by packing of the dehydrated samples in a polycrystalline receptacle and spectra collected on a Perkin Elmer model 2000 FT-IR Raman Spectrometer, fitted with a quartz beam splitter and an indium gallium arsenide (InGaAs) detector. The excitation source was a Spectron Laser Systems SL301 Nd–YAG laser emitting at a wavelength of 1064 nm. Stokes-scattered radiation was collected over an effective Raman shift range of 3800–200 cm^{-1}, with an instrumental resolution of 8 cm^{-1}. A laser power of 100 mW was used with the co-addition of 120 scans to give a high signal-to-noise ratio.

The dehydrated samples were analysed by X-ray diffraction (XRD) using a PHILIPS PW1050 diffractometer with a Long Fine Focus Co-Kα radiation source at 40 kV and 40 mA. The LFF Co source had 1° divergence, 1° anti-scatter, 0.2 mm receiving slit and 1 set of solar slits. The samples were presented as a thin film by mechanical treatment of the dehydrated samples, dissolved in a minimum of ethanol and adhered to a thin glass plate. Diffraction patterns were collected from 12°–65° 2θ with a 0.02° step at a speed of 0.2° min^{-1}, and analysed and refined using Diffraction Technology Traces 6.1.3.

Table 1 Preparation conditions of nanocrystalline TiO_2 samples

Sample	Treatment conditions
S1	(i) Tetraisopropyltitanate in isopropanol added to excess water (ii) HNO_3, heat at 80 °C with stirring for 8 hours
S2	S1, 15 hours 200 °C, autoclave Parr-bomb, convection oven
S3	S1, 30 psi (121.5 °C), 2 minute ramp, TAP 10 minutes, 80% 630 W microwave oven
S4	S1, 60 psi (145 °C), 2 minute ramp, TAP 5 minutes, 80% 630 W microwave oven

The morphology and grain size of particles were determined using transmission electron microscopy (TEM) on a PHILIPS CM200 Analytical Scanning Transmission Electron Microscope operating at 200 kV. The samples were diluted with ethanol and presented on a copper grid. Electron diffraction patterns were obtained following the TEM measurements.

Results and discussion

The preparation conditions, for samples S1–S4 are summarized in Table 1.

The standard industrial and research based procedure for identification and classification of TiO_2 colloids involves crystalline phase assignment and an approximation of particle size and distribution. Conventionally this involves the use of powder X-ray diffraction (XRD) and transmission electron microscopy (TEM). We have further characterized our samples using Raman spectroscopy allowing the measurement of relative crystallinity and the weighting of the particle size distribution.

The XRD traces obtained for S1–S4 (Fig. 1) were compared to the database standard PDF 21-1272 and the phase identified as being anatase. An unidentified reflection at 35° 2θ can be attributed to the presence of brookite, PDF 29-1360, in small proportions. It has been demonstrated that crystallite sizes for metal oxides can be determined using the Scherrer equation [eqn. (1)].[9]

$$B(2\theta) = \frac{0.94\lambda}{L\cos\theta} \quad (1)$$

The reflections characteristic for anatase were used to determine the relative crystallite sizes for each of the samples

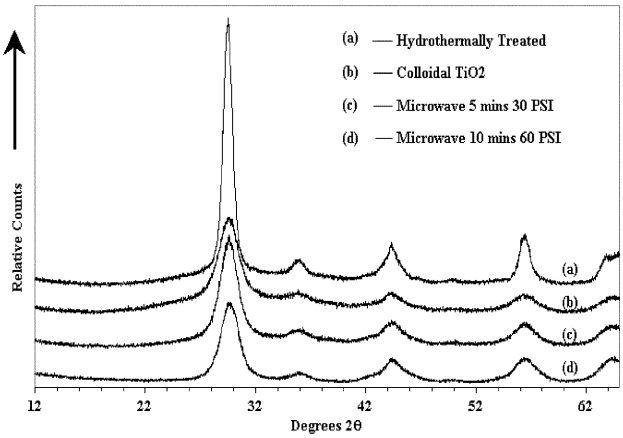

Fig. 1 XRD traces of titania colloids: a) S1, b) S2, c) S3, d) S4.

Table 2 Calculated crystallite sizes (nm) from XRD patterns

Sample	29.58/° 2θ
S1	3.4
S2	10.2
S3	4.8
S4	4.8

where $B(2\theta)$ is the linewidth, θ is the peak position and L is the crystallite size in nanometers. Table 2 outlines the calculated crystallite sizes.

The peak intensity in XRD can be correlated both to the amount of crystalline material that is subjected to the source and to the crystallite size. A sharp intense peak corresponds to larger particles with a high number of defect crystalline planes while broad weak peaks conversely correspond to small particles of highly crystalline material. To relate these properties through a series of samples the peaks' full width at half maximum (FWHM) are compared. Thus, examining the data closely a trend can be seen both in the XRD traces and in the calculated crystallite size. This corresponds to the defect crystalline material in S1 undergoing high-pressure, high-temperature recrystallisation in the hydrothermal samples to form a highly crystalline material. Distinct similarities between S2 and S3 (or S4) can be seen indicating a high degree of crystallinity. However, the microwave treated samples remain as small (3–5 nm) relatively monodispersed nanocrystallites, while the convection treated samples grow in size (10 nm). This result is thought to be linked to the very fast rate of recrystallisation kinetics in these samples allowing no significant growth in the nanocrystallites.[5]

TEM images supported the calculated particle size from the XRD data for each sample. Fig. 2 is the TEM image of S1 in which no hydrothermal treatment was carried out. The particles had a wide size distribution in the 3–35 nm range with irregular nanocrystallite shapes. It is noted that the calculated nanocrystallite size from the XRD data was significantly smaller. This observation is attributed to the fact that the Scherrer equation calculates an average crystallite size, and the colloidal TiO_2 clearly has a wide size distribution. The Scherrer equation therefore predicts that the colloidal sample, S1, has a particle size distribution that is centred on the smaller 3–6 nm size.

By comparison, the image of the convection hydrothermally treated sample (S2) in Fig. 3 shows a more homogeneous particle distribution. The TEM image of S2 depicts crystalline particles with a particle size distribution of approximately 10–15 nm. This image corresponds to the calculated crystallite size from XRD data and also demonstrates visually that hydrothermal treatment produces a more regular crystalline material with a narrower particle size distribution.

Fig. 2 TEM image of S1, colloidal TiO_2 suspension.

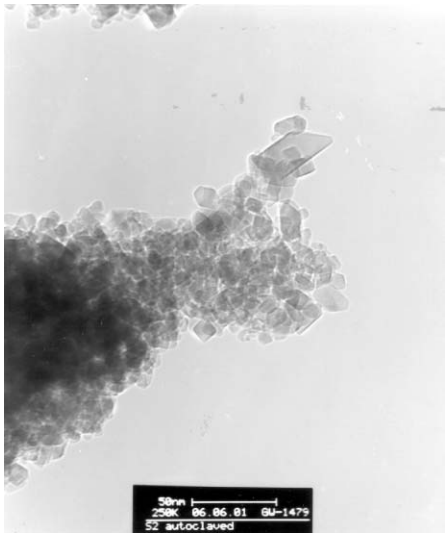

Fig. 3 TEM image of S2, convection hydrothermally treated TiO_2 colloids.

The TEM analysis of the microwave hydrothermally treated titania colloids is given in Fig. 4. The image was obtained under difficult operating conditions with the relative particle size leading to contrast difficulties. This was suggested to be a result of the particles on the polymeric support of the TEM copper grid being smaller in diameter than the thickness of the film, thus making it difficult to focus a clear image of the particles. Although the image is not highly defined, the observable crystalline material can be scaled to be approximately 5 nm. It can also be observed that the sample has a narrow size distribution of crystalline particles.

An advantage of using TEM as an analysis tool is the possibility of obtaining electron diffraction patterns. This proved invaluable in this work since the particle size and crystallinity were thought to be the keys for use of these materials in electrochemical devices.

An electron diffraction pattern was obtained for the convection hydrothermally treated sample, S2. Fig. 5 shows the database standard for anatase and brookite overlayed across

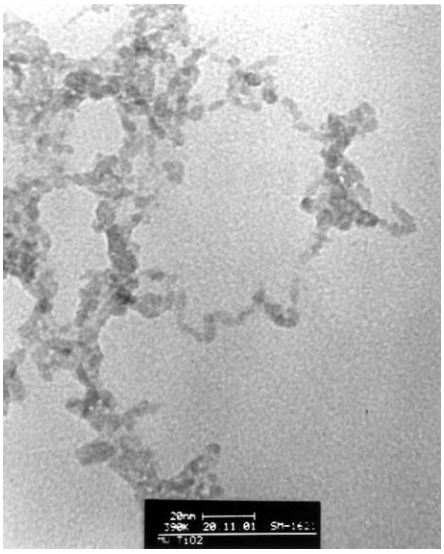

Fig. 4 TEM image of S3, microwave hydrothermally treated TiO_2 colloids.

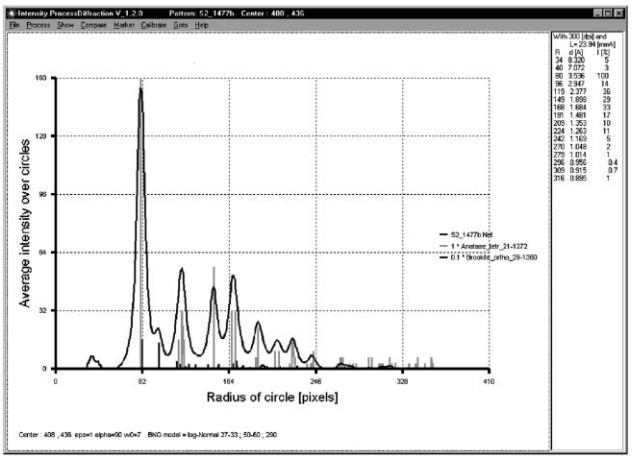

Fig. 5 Electron diffraction pattern of S2, convection hydrothermally treated TiO_2. Comparison of XRD intensity to database standard PDF 21-1272 (anatase) and PDF 26-1360 (brookite).

the measured diffraction pattern and the associated ring intensity. The ring structure of the electron diffraction pattern indicates that the material being analysed is crystalline and the diffraction pattern obtained was matched to a database standard for anatase. However, a bright ring is observed as the third concentric circle. This gave evidence to support the presence of brookite as a transition phase present in the processed material and was analysed further. The relative intensity of the ring structure was compared to database standards for both anatase and brookite. The generated intensities from the electron diffraction pattern indicated that the sample contained a small proportion of brookite as a phase mixture in less than 0.1% of the sample.

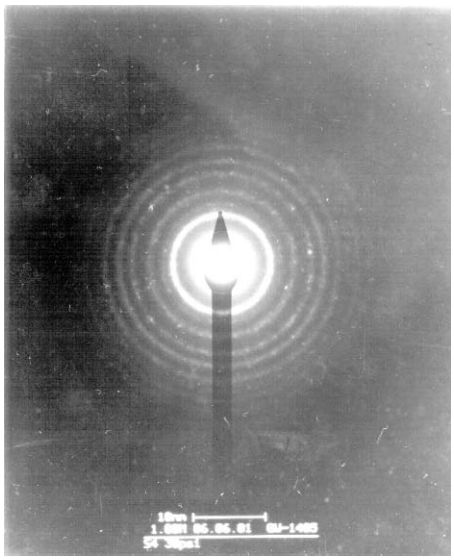

Fig. 6 Electron diffraction pattern for S4, microwave hydrothermally treated TiO_2.

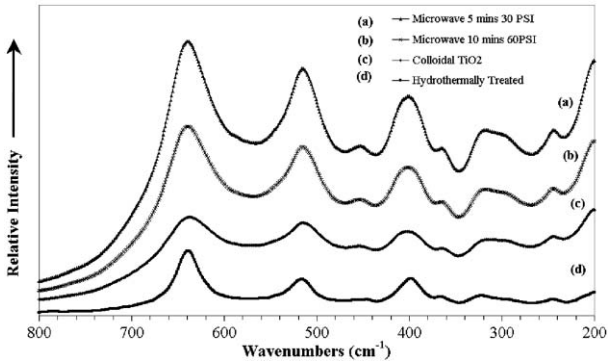

Fig. 7 Raman spectra of TiO_2 nanocrystallites: a) S1, b) S4, c) S3, d) S2.

For comparison, an electron diffraction pattern for the microwave hydrothermally treated sample, S3, was obtained and compared to that obtained for S2 and is shown in Fig. 6.

Similarities in the diffraction patterns between the convection and microwave hydrothermally treated samples were observed with ring structures and *d* spacings being comparable. A significant difference between the samples was that the microwaved sample produced a pattern of diffraction dots and not clearly defined rings. This indicates that the crystallites of the microwave hydrothermally treated material were more highly crystalline than that of the convection treated sample. This is a significant result in that the time and energy taken to produce a more highly crystalline material is significantly less, *i.e.* 544 W microwave for 12 minutes compared to a 1300 W oven for 15 hours.

Further analysis was undertaken of the nanocrystalline colloidal titania using Raman spectroscopy. The four spectra were obtained as discussed previously and are shown in Fig. 7.

The features determined by XRD and TEM for each of the four samples can be observed as trends in the Raman spectrum for each titania sample. The information available from a Raman spectrum is extremely valuable from a comparison standpoint. Such information includes an increase in relative intensity of peaks in the Raman spectrum, indicating an increase in the relative crystallinity of the material. Further, vibrational modes such as the A_{1g} and E_g modes, indicative of crystal lattice vibrations, are observed to shift to higher energy with a decrease in peak width that indicates an increase in the crystallinity of the particles being analysed.[10,11] Several features that are also noteworthy in relation to nanocrystalline semiconductors have been identified by Doss and Zallen,[9] and include the implication that an increased low-frequency wing for a Raman band correlates to a particle size distribution that is centred on the small-particle side of the distribution.

Considering the spectrum shown in Fig. 7 the bands at 514 and 639 cm^{-1} correspond to A_{1g} and E_g modes respectively.[10] The region between 200 and $\sim$360 cm^{-1} has been identified with peaks associated with the presence of brookite, which is supported by the XRD and electron diffraction data discussed earlier. To summarise the data from Fig. 7 the calculated peak widths at half height are shown in Table 3.

Table 3 Relative peak widths for identified anatase Raman bands

Sample	Characteristic	E_g	A_{1g}–B_{1g}	B_{1g}
S1	Peak height	26.1	21.7	14.9
	Normalised peak width ½ height	1.71 cm^{-1}	1.70 cm^{-1}	2.14 cm^{-1}
S2	Peak height	39.8	17.1	17.9
	Normalised peak width ½ height	0.68 cm^{-1}	1.57 cm^{-1}	1.36 cm^{-1}
S3	Peak height	90.6	68.8	45.9
	Normalised peak width ½ height	0.57 cm^{-1}	0.50 cm^{-1}	0.70 cm^{-1}
S4	Peak height	63.8	47.3	30.8
	Normalised peak width ½ height	0.69 cm^{-1}	0.74 cm^{-1}	1.05 cm^{-1}

The key points to note from Fig. 7 and Table 3 are that S1, the control sample, exhibits a weak peak intensity that is broad in appearance. Distinct peak asymmetry can be observed with the low-frequency wing in much larger proportion than with the high-frequency wing, indicating a spread in the particle distribution that is skewed towards the smaller particle size.

The microwave hydrothermally treated sample, S3, in comparison to S1, shows an increase in peak intensity while the peak width has narrowed. The Raman band corresponding to an E_g vibrational mode can also be observed to shift to higher energy indicating an increase in crystal lattice vibration energy and therefore an increase in crystallinity. An increase in peak symmetry can be observed compared to S1, indicating a narrower particle size distribution centred on the smaller sized particles.

The microwave hydrothermally treated sample S4 shows similar features to that of S3. Specifically, a relative increase in peak intensity is observed with a narrowing peak width and a shift to higher energy. An increase in peak symmetry has also been measured indicating a narrow distribution of small particles.

The convection hydrothermally treated sample, S2, exhibits intense narrow peaks coupled with a shift to higher energy of the crystal lattice vibration modes. The E_g mode does not exhibit a low-frequency wing and the peak is symmetrical indicating the sample has a narrow particle size distribution.

Throughout the series, comparisons of the normalised peak widths at half height in the Raman spectrum can be used as an indicator of the relative crystallinity, with a smaller value relating to a more regular crystalline structure. A definite trend is therefore observed in the normalised peak widths at half height in which untreated samples have larger values indicating a more disordered crystalline structure. Comparison of the two hydrothermally treated samples indicates that the microwave hydrothermally treated sample, S3, has a more crystalline structure than that of the convection hydrothermally treated sample S2.

Conclusions

The data presented indicate that the use of microwave hydrothermal processing of colloidal TiO_2 solutions allowed for rapid heating to temperature and extremely rapid kinetics of recrystallisation.[5] This results in a highly nanocrystalline material with a narrow size distribution in the range of 4–5 nm.

The implications of this technique will provide faster processing time for obtaining a more crystalline material with a smaller size and a more regular shape. The processing method may have significant implication for both the processing of nanocrystalline particles for electrochemical applications and the efficiency of their function within these devices.

Acknowledgement

The authors acknowledge the Analytical Electron Microscopy Facility at Queensland University of Technology for its assistance with TEM, electron diffraction and X-ray diffraction analysis. This work was financially supported by the Centre for Instrumental and Developmental Chemistry at Queensland University of Technology.

References

1 P. A. Venz, J. T. Kloprogge and R. L. Frost, *Langmuir*, 2000, **16**(11), 4962–4968.
2 P. A. Venz, R. L. Frost, J. R. Bartlett and J. L. Woolfrey, *Spectrochim. Acta, Part A*, 1997, **53**(7), 969–977.
3 B. O'Regan and M. Graetzel, *Nature, 1991*, 6346, **353**, 737–740.
4 R. Cinnsealach, G. Boschloo, N. S. Rao and D. Fitzmaurice, *Sol. Energy Mater. Sol. Cells*, 1999, **57**(2), 107–125.
5 S. Komarneni, R. K. Rajha and H. Katsuki, *Mater. Chem. Phys.*, 1999, **60**(1), 50–54.
6 J. Ayllon, A. Piero, E. Vigil, X. Domenech and J. Pearl, *J. Mater. Chem.*, 2000, **10**, 1911–1914.
7 M. Graetzel, *Prog. Photovoltaics*, 2000, **8**(1), 172–185.
8 B. O'Regan, J. Moser, M. Anderson and M. Graetzel, *J. Phys. Chem.*, 1991, **94**(24), 8720–8726.
9 C. J. Doss and R. Zallen, *Phys. Rev. B: Condens. Matter*, 1993, **48**(21), 15626–15637.
10 H. Cheng, J. Ma, Z. Zhao and L. Qi, *Chem. Mater.*, 1995, **7**(4), 663–671.
11 R. J. Betsch, H. L. Park and W. B. White, *Mater. Res. Bull.*, 1991, **26**(7), 613.